

# Improve power conversion efficiency of slab coupled optical waveguide lasers

Jiahua Fan,<sup>1,\*</sup> Lin Zhu,<sup>1</sup> Mehmet Dogan,<sup>2</sup> and Jonah Jacob<sup>2</sup>

<sup>1</sup>Department of Electrical and Computer Engineering, Center for Optical Material Science and Engineering Technologies, Clemson University, Clemson, South Carolina 29634, USA

<sup>2</sup>Science Research Laboratory, Inc., 15 Ward St., Somerville, MA 02143, USA

\*[jiahuaf@clemson.edu](mailto:jiahuaf@clemson.edu)

**Abstract:** The slab coupled optical waveguide laser (SCOWL) is a promising candidate for high power, single mode emitter for a number of reasons, including its near diffraction limited optical quality, large modal size and near circular output pattern. Current SCOWL designs have limited electrical-optical power conversion efficiency (PCE) around 40%, which is lower than conventional RWG laser and broad area laser that are known to have much higher PCEs. To improve the SCOWL PCE, we theoretically optimize its structure by reducing Al content, increasing doping concentration and introducing a GRIN layer to prevent carrier leakage. Numerical simulations predict that an optimized SCOWL design has a maximum PCE of about 57% at room temperature.

© 2014 Optical Society of America

**OCIS codes:** (140.5960) Semiconductor lasers; (140.3570) Lasers, single-mode.

---

## References and links

1. E. S. Kintzer, J. N. Walpole, S. R. Chinn, C. A. Wang, and L. J. Missaggia, "High-power, strained-layer amplifiers and lasers with tapered gain regions," *IEEE Photon. Technol. Lett.* **5**(6), 605–608 (1993).
2. M. Mikulla, P. Chazan, A. Schmitt, S. Morgott, A. Wetzel, M. Walther, R. Kiefer, W. Pletschen, J. Braunstein, and G. Weimann, "High-brightness tapered semiconductor laser oscillators and amplifiers with low-modal gain epilayer-structures," *IEEE Photon. Technol. Lett.* **10**(5), 654–656 (1998).
3. B. Sumpf, K. H. Hasler, P. Adamiec, F. Bugge, F. Dittmar, J. Fricke, H. Wenzel, M. Zorn, G. Erbert, and G. Tränkle, "High-brightness quantum well tapered lasers," *IEEE J. Sel. Top. Quantum Electron.* **15**(3), 1009–1020 (2009).
4. A. Knauer, G. Erbert, R. Staske, B. Sumpf, H. Wenzel, and M. Weyers, "High-power 808 nm lasers with a super-large optical cavity," *Semicond. Sci. Technol.* **20**(6), 621 (2005).
5. J. P. Donnelly, R. K. Huang, J. N. Walpole, L. J. Missaggia, C. T. Harris, J. J. Plant, R. J. Bailey, D. E. Mull, W. D. Goodhue, and G. W. Turner, "Algaas-ingaas slab-coupled optical waveguide lasers," *IEEE J. Quantum Electron.* **39**(2), 289–298 (2003).
6. R. K. Huang, J. P. Donnelly, L. J. Missaggia, C. T. Harris, B. Chann, A. K. Goyal, A. S. Rubio, T. Y. Fan, G. W. Turner, "High brightness slab-coupled optical waveguide lasers," *Proc. SPIE* **6485**, 64850F (2007).
7. R. K. Huang, L. J. Missaggia, J. P. Donnelly, C. T. Harris, and G. W. Turner, "High-brightness slab-coupled optical waveguide laser arrays," *IEEE Photon. Technol. Lett.* **17**(5), 959–961 (2005).
8. G. M. Smith, J. P. Donnelly, L. J. Missaggia, M. K. Connors, S. M. Redmond, K. J. Creedon, D. C. Mathewson, R. B. Swint, A. S. Rubio, G. W. Turner, "Slab-coupled optical waveguide lasers and amplifiers," *Proc. SPIE* **8241**, 8241S (2012).
9. C. Lauer, H. König, G. Grönninger, S. Hein, A. G. Iglesias, M. Furlitsch, J. Maric, H. Kissel, P. Wolf, J. Biesenbach, U. Strauss, "Advances in performance and beam quality of 9xx-nm laser diodes tailored for efficient fiber coupling," *Proc. SPIE* **8241**, 824111 (2012).
10. P. Crump, M. Grimshaw, J. Wang, W. Dong, S. Zhang, S. Das, J. Farmer, and M. DeVito, "85% power conversion efficiency 975-nm broad area diode lasers at-50 C, 76% at 10 C," in *Quantum Electronics and Laser Science Conference*, Optical Society of America, JWB24 (2006).

11. M. Kanskar, T. Earles, T. J. Goodnough, E. Stiers, D. Botez, and L. J. Mawst, "73% CW power conversion efficiency at 50 W from 970 nm diode laser bars," *Electron. Lett.* **415**, 245–247 (2005).
  12. G. M. Smith, R. K. Huang, J. P. Donnelly, L. J. Missaggia, M. K. Connors, G. W. Turner, and P. W. Juodawlkis, "High-power slab-coupled optical waveguide lasers," *Proc. IEEE Photon. Soc. Annu. Meet.*, 479–480 (2010).
  13. LASTIP, Crosslight Software Inc., Canada.
  14. H. Wenzel, P. Crump, A. Pietrzak, X. Wang, G. Erbert, and G. Tränkle, "Theoretical and experimental investigations of the limits to the maximum output power of laser diodes," *New J. Phys.* **12**(8), 085007 (2010).
  15. P. W. Juodawlkis, J. J. Plant, W. Loh, L. J. Missaggia, F. J. O'Donnell, D. C. Oakley, A. Napoleone, J. Klamkin, J. T. Gopinath, D. J. Ripin, S. Gee, P. J. Delfyett, and J. P. Donnelly, "High-Power, Low-Noise 1.5- $\mu\text{m}$  Slab-Coupled Optical Waveguide (SCOW) Emitters: Physics, Devices, and Applications," *IEEE J. Sel. Top. Quantum Electron.* **17**(6), 1698–1714 (2011).
  16. H. Hirayama, Y. Miyake, and M. Asada, "Analysis of current injection efficiency of separate-confinement-heterostructure quantum-film lasers," *IEEE J. Quantum Electron.* **81**, 68–74 (1992).
- 

## 1. Introduction

Laser diodes (LDs) have been widely used for many industrial and scientific applications because of their high PCEs, compactness and brightness. Several critical applications, such as pump sources for fiber and solid state laser systems, usually require high output power and particularly for fiber lasers, high brightness. The conventional single mode ridge waveguide laser (RWG) has an excellent beam quality but cannot provide high output power due to its relatively small modal size, which results in a low threshold for catastrophic optical damage (COD). To overcome the power limitation of conventional single mode LDs, various approaches have been proposed to expand the mode size, including tapered laser [1–3], super large optical cavity laser [4], and slab-coupled optical waveguide laser (SCOWL) [5–8]. Among the various single mode lasers, SCOWs offer unique advantage of a nearly circular output pattern and therefore is a great candidate for providing both high output power and brightness resulting in efficient coupling into fibers.

Compared with the RWG laser, the SCOWL has an expanded n-doped waveguide slab layer and wider rib width. The materials and layer dimensions of SCOWs are properly chosen so that the fundamental mode of the ridge waveguide is coupled with the fundamental slab mode, resulting in an expanded mode profile. The lateral confinement for the SCOWL mode is provided by the etched ridge, while higher order modes leak through the slab layers and exhibit much larger losses. The power-conversion-efficiency (PCE) for current SCOWL designs is only around 40% at high power, which is much lower than the PCE of state-of-art RWG lasers (around 60%) and broad area lasers (over 70% [9–11]) at 980nm. The power that is not converted into light results in waste heat which increases the operation temperature and generates deleterious effects including a thermal roll-over of the PCE. In other words, the low PCE of the SCOWL also limits the maximum output power.

In this work, we optimize the SCOWL design with a goal of improving its PCE. The analysis of power distribution in a typical SCOWL design predicts that a large portion of the input electrical power is lost due to the series resistance and the threshold current. Although the relatively large threshold current is inevitable because of its weak confinement nature, one can reduce the series resistance by reducing the overall Aluminum composition and increasing the doping concentration. In addition, a GRIN layer is added to the p-doped side to prevent carrier leakage. As we will present later, such a design results in a maximum PCE~57% at room temperature.

## 2. Quantification of the various inefficiencies

In the early SCOWL design, the active region was placed inside the rib to enhance the lateral confinement and ensure the single mode operation. However, etching through the quantum wells (QWs) usually generated surface defects that led to additional surface states and decreased

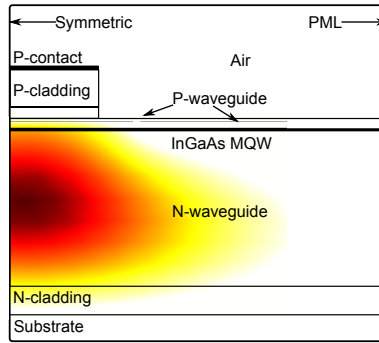


Fig. 1. The cross-section of the simulated SCOWL device. Only half of the structure is included in the simulation because of the symmetrical plane on the left boundary. A perfect match layer (PML) is placed on the right boundary of the simulation window to damp high order leaky modes.

the efficiency of photon generation in the wells. It has been reported that placing the active layer inside the slab region to eliminate etching process of QWs improve both the efficiency and reliability of the device [12]. Thus, we will not etch through QWs in our designs. Figure 1 is a schematics of the simulated 980nm SCOWL. The materials chosen for each layer are similar with the reported design by MIT Lincoln Laboratory [5]. The active region contains three InGaAs QWs separated by GaAsP barrier layer.

The optical output power and bias voltage were numerically calculated by using the commercial laser simulation tool, LASTIP [13]. The two dimensional carrier transport is simulated based on the drift-diffusion model. An empirical model of the free carrier absorption is also included to accurately estimate the internal optical loss [14]. The device was assumed to be at room temperature.

The simulated current-voltage (V-I) and power-current (L-I) characteristics for SCOWL design 1 (Table 1) are shown in Fig. 2. Other than the output optical power (P), part of the electrical power is converted into waste heat during laser operation due to (a) the threshold current, (b) the

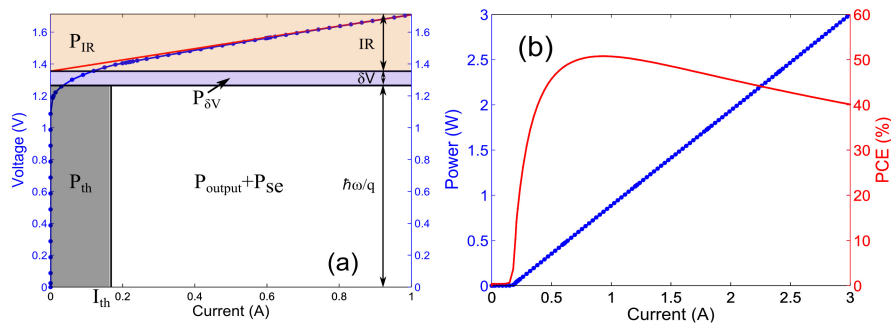


Fig. 2. (a) Simulated I-V characteristics for SCOWL design 1. The blue dotted line corresponds to the simulated data points, and the red line shows the linear fitting at 1A to obtain the series resistance and turn-on voltage.  $I_{th}$  stands for the threshold current. The areas of the rectangles correspond to the power distribution (see details in the context). The length of the laser is 3mm. The width of the rib is  $4.5\mu\text{m}$  for all the designs in this study. The reflectivity is 32% on both facets. (b) The calculated L-I curve and PCE.

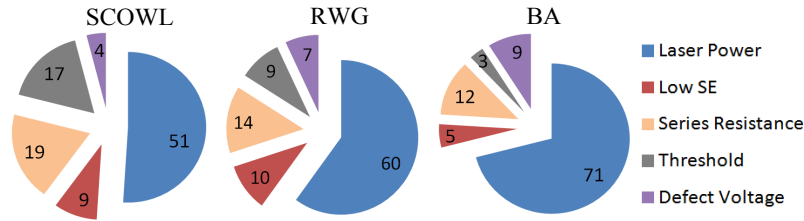


Fig. 3. Power distribution calculated based on the simulation result for SCOWL, RWG and BA lasers.

excess bias voltage, and (c) the optical/electrical losses. The excess electrical voltage is a result of the voltage defect and device series resistance. Throughout the simulation, we have assumed good ohmic contacts at the metal-semiconductor interfaces without additional Schottky barrier. On the other hand, only the injected current above the threshold contributes to optical output. Therefore, it allows us to divide the total electrical power into four parts as presented in Fig. 2(a). The device resistance ( $R$ ) equals to the slope of V-I curve, which is obtained by a linear extrapolation around 1A. The intercept of the extrapolated line (shown in red) with the Voltage Axis corresponds to the turn-on voltage of the laser. The difference between the turn-on voltage and the photon voltage ( $\hbar\omega/q$ ) is defined as the voltage defect ( $\delta V$ ), which is mainly due to the interface voltage in our simulation. As shown in Fig. 2(a), the three parts in the colored regions correspond to power lost due to, (a) the threshold current ( $P_{th} = I_{th}\hbar\omega/q$  as colored in gray), (b) the series resistance ( $P_R = I^2R$  as colored in orange) and (c) the voltage defect ( $P_{\delta V} = \delta VI$  as colored in violet), respectively. The remainder is the maximum output laser power with an ideal slope efficiency. In reality, the slope efficiency of the device is lower than the theoretical maximum because of the optical losses and non-radiative electron-hole recombination losses. We define the difference as the power lost resulting from the non-ideal slope efficiency ( $P_{se}$ ).

This SCOWL design works well without the lowering of slope efficiency for up to 3A (Fig. 2(b)). However, the PCE is only 50% at its maximum and decreases to around 40% at higher input. To understand the causes of this limited PCE, the power distribution is calculated and compared to the results for a typical broad area (BA) laser and a typical RWG laser operating at the same wavelength in Fig. 3. The data presented are obtained with the same inject current density for the three lasers. Apparently, more electrical power is lost due to higher threshold current and series resistance in the SCOWL. Because the SCOWL mode is expanded and pushed into the n-doped slab region, the overlap between optical field and the active region is very low (typically around 0.5%), which results in the relatively large threshold current. The series resistance comes from both the contribution of Al in the material and the large overall thickness of lightly doped waveguide layers. Since the expansion of mode size is the very essence of SCOWL, we mainly focused on reducing the resistance in this study.

### 3. Improved design for high efficiency

Because the electrical conductivity decreases with the Al composition in AlGaAs, one way to reduce the bulk resistance of the device is to use less aluminum. However, for a InGaAs/AlGaAs laser operating around  $1\mu\text{m}$ , a sufficiently high Al composition is usually required to ensure carrier confinement in the active region. The calculated L-I characteristics and PCE shown in Fig. 4(a) corresponds to the SCOWL design 2 where the overall Al composition is reduced by about 5% in all the layers from design 1. The overall series resistance is therefore reduced from  $0.39\Omega$  to  $0.25\Omega$  at 1A. The practical series resistance values depend on the device dimensions. The calculated value of the base design is comparable to the experimental results for

Layer	Material	Design 1			Design 2			Design 3		
		Thickness [nm]	Doping [ $10^{18}\text{cm}^{-3}$ ]	Al (x)	Thickness [nm]	Doping [ $10^{18}\text{cm}^{-3}$ ]	Al (x)	Thickness [nm]	Doping [ $10^{18}\text{cm}^{-3}$ ]	Al (x)
P-contact	GaAs	120	2	-	120	2	-	120	2	-
P-cladding	$\text{Al}_x\text{Ga}_{1-x}\text{As}$	1600	0.2 to 1	0.25	1300	0.2 to 1	0.2	1300	2	0.2
P-waveguide	$\text{Al}_x\text{Ga}_{1-x}\text{As}$	200	0.1	0.2	200	0.2	0.15	200	1	0.15 to 0.17
P-waveguide	$\text{Al}_x\text{Ga}_{1-x}\text{As}$	-	-	-	200	0.1	0.15	100	0.5 to 1	0.15
P-waveguide	$\text{Al}_x\text{Ga}_{1-x}\text{As}$	-	-	-	-	-	-	100	-	0.15
Active	InGaAs MQW	69	-	-	48	-	-	48	-	-
N-waveguide	$\text{Al}_x\text{Ga}_{1-x}\text{As}$	3800	0.05 to 0.1	0.2	3800	0.05 to 0.1	0.15	3800	0.05 to 0.1	0.15
N-cladding	$\text{Al}_x\text{Ga}_{1-x}\text{As}$	1700	0.1 to 2	0.25	1700	0.1 to 2	0.2	1700	0.1 to 2	0.2
Substrate	GaAs	-	2	-	-	2	-	-	2	-

Table 1. Layer structures of three SCOWL designs.

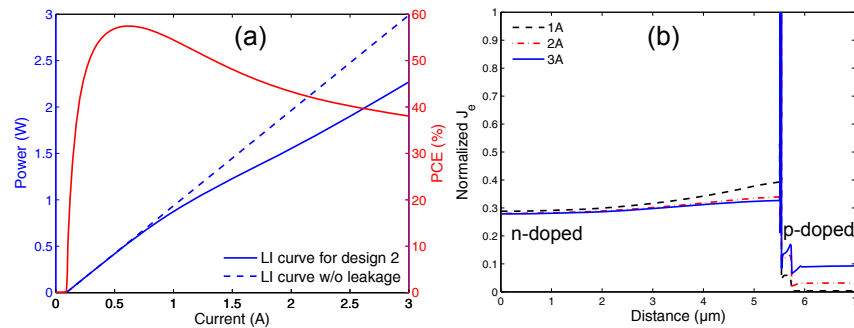


Fig. 4. (a) Calculated L-I curve and PCE for design 2. The blue dotted line shows a linear fitting near threshold. (b) Electron current density ( $J_e$ ) distribution along the vertical direction at the center of the device from n-contact to p-contact for different input currents.

SCOWLS in Ref. [15] if we scale the series resistance linearly with the device length. Although the maximum value of PCE is increased, it rapidly decreases with current. This is mainly due to the electron leakage into the p-doped region. Figure 4(b) plots the normalized electron current density ( $J_e$ ) distribution along the vertical direction as increasing the input current. On the left side of the multiple quantum wells (MQW), the decrease of the normalized  $J_e$  is due to current spreading. On the right side of the MQW, the electron leakage occurs above the threshold and gets more severe at higher injection current (bias voltage). Because electrons lost to leakage recombine with holes in the p-side layers instead of in the quantum well, the quantum efficiency decreases dramatically which is reflected in the decreased slope efficiency. Comparing the L-I curve to the dotted line which is plotted by a linear extrapolation near threshold in Fig. 4(a), the output power is reduced by about 25% due to carrier leakage. We use the band diagram to further examine the electron leakage problem. Under an external bias, the potential barrier for electrons from the quantum well to p-waveguide layer is similar to a finite triangular potential barrier, as shown in Fig. 5 and its inset. The tunneling probability for electrons to travel through the potential barrier depends on both the width and height of the barrier. When the lower Al composition is introduced in the waveguide layer, the barrier height decreases. On the other hand, as the bias voltage keeps increasing, the conduction band in the p-waveguide layer bends due to the excess potential, which causes the shrinkage of the width of the triangular potential. To postpone the onset of carrier leakage, we can add a graded index (GRIN) layer between the waveguide and cladding layers [16]. Because the bandgap energy gradually increases with the distance from the well in the GRIN layer, it can partially compensate the bending of the conduction band under the excess bias voltage. The effective width of the potential barrier for

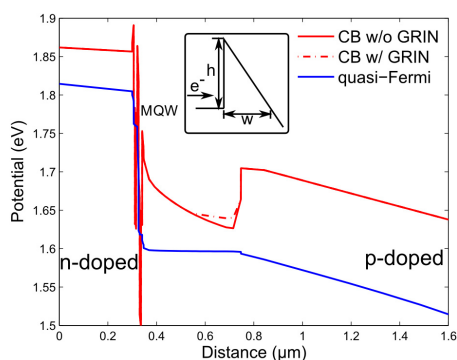


Fig. 5. Band diagram under certain bias voltage for the SCOWL design 2 with and without GRIN layer. The red lines are the conduction band (CB) and the blue line is the quasi-Fermi level. The inset illustrates a triangular potential barrier that electrons encounters when traveling through the p-waveguide layer.

electrons increases, resulting in a reduced carrier leakage.

Increasing the impurity doping also reduces electrical resistance. Usually this is not preferred because the internal optical loss increases with the doping concentration due to free carrier absorption. However, it is feasible to increase the doping on the p-side in the SCOWL, thanks to the small overlap between the optical mode and the lossy p-doped region. Additionally, increasing the doping concentration on the p-side is more effective than on the n-side with regard to reducing the resistance, because most of the series resistance is generated in the p-doped layers because of the much smaller mobility of holes.

Based on the concepts discussed above, we modify the layer thickness, etching depth, doping profile and material composition of the original SCOWL design and results in an optimized combination for maximizing the PCE. The layer structures of the optimized SCOWL (design 3) are listed in Table 1. A GRIN layer is inserted to help eliminate carrier leakage for injected current up to 3A. Since the total thickness of the high-index p-waveguide layers increases in the optimized design, the optical mode moves upwards and the confinement factor tends to increase. This can be seen from the far field profile in Fig. 6. Compared with the original

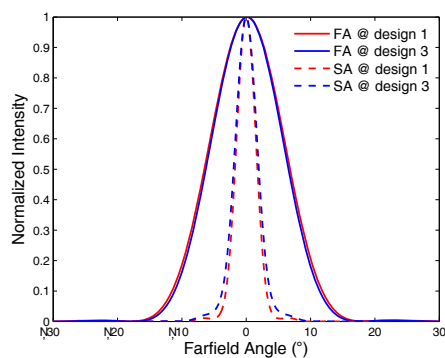


Fig. 6. The farfield profile along fast axis (FA) and slow axis (SA) for design 1 and design 3.

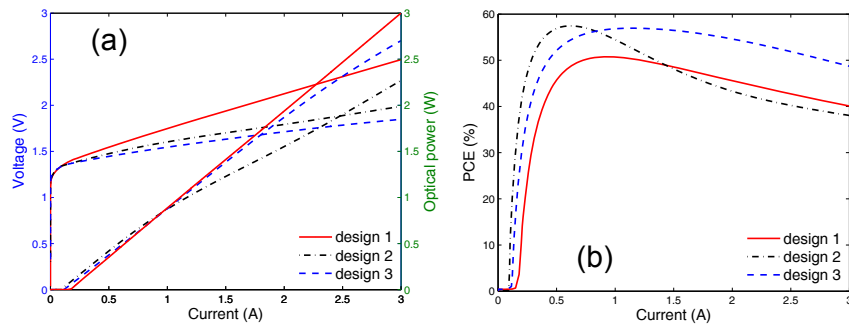


Fig. 7. (a) The simulated L-I-V curves for the three designs listed in table 1. (b) The calculated PCE versus current curves for the three designs.

design 1, the beam divergence angle along the slow axis (horizontal) increases from  $3.4^\circ$  to  $3.9^\circ$  at full width at half maximum (FWHM) and from  $6.6^\circ$  to  $8.6^\circ$  for 95% power content, while the divergence angles along the fast axis are almost unchanged and are about  $12.4^\circ$  (FWHM) and  $20.6^\circ$  (95% content). The increase of the confinement factor also tends to increase the modal gain. Because the SCOWL supports multiple waveguide modes, it is important to keep the modal gain small enough during operation so that higher modes will not reach threshold. Therefore, we reduced the number of quantum wells in the active region from three to two to keep the confinement factor lower for better modal discrimination. This also reduces the interface voltage by about 0.08eV.

The simulated L-I-V and PCE curves for the optimized design are shown in Fig. 7(a) and 7(b). Also shown in this Figure are the comparisons with the results from other two designs. By increasing the doping concentration and reducing the Al composition, the overall series resistance of the laser structure is reduced to  $0.19\Omega$  at 1A, which is about 50% of its value in design 1. We estimate that the doping profile and Al composition changes contribute approximately equally to the reduction of the series resistance. By adding the GRIN layer and reducing the excess voltage, the carrier leakage is very small during the simulation. Despite the slightly reduced slope efficiency due to higher doping, the optimized design shows an improved PCE at about 57% because of the much reduced series resistance. The optimized SCOWL design also exhibits the similar PCE with the RWG laser at watt-level output power.

#### 4. Conclusion

We simulated and optimized the SCOWL design for high PCE at watt-level output. The power analysis of the non-lasing losses shows that the original design has limited PCE because of the excess voltage and the higher threshold current. The excess voltage is reduced by lowering the overall Al content and increasing doping concentration on the p-doped region. A GRIN layer inserted on the p-side also helps to prevent electron leakage under bias voltage. The maximum PCE has been increased to 57% at room temperature.